Observational evidence for variations of the acoustic cutoff frequency with height in the solar atmosphere

A. Wiśniewska[1], Z.E. Musielak[2,1],J. Staiger[1] and M.Roth[1]

[1]*Kiepenheuer-Institut für Sonnenphysik,*

Schöneckstr. 6, D-79104 Freiburg, Germany

[2]*Department of Physics, University of Texas at Arlington,*

Arlington, TX 76019, USA

wisniewska@kis.uni-freiburg.de; zmusielak@uta.edu;
staiger@kis.uni-freiburg.de;mroth@kis.uni-freiburg.de

ABSTRACT

Direct evidence for the existence of an acoustic cutoff frequency in the solar atmosphere is given by observations performed by using the HELioseismological Large Regions Interferometric DEvice operating on the Vacuum Tower Telescope located on Tenerife. The observational results demonstrate variations of the cutoff with atmospheric heights. The observed variations of the cutoff are compared to theoretical predictions made by using five acoustic cutoff frequencies that have been commonly used in helioseismology and asteroseismology. The comparison shows that none of the theoretical predictions is fully consistent with the observational data. The implication of this finding is far reaching as it urgently requires either major revisions of the existing methods of finding acoustic cutoff frequencies or developing new methods that would account much better account for the physical picture underlying the concept of cutoff frequencies in inhomogeneous media.

Subject headings: Sun: atmosphere — hydrodynamics — waves

1. Introduction

The existence of an acoustic cutoff frequency on the Sun has far-reaching consequences because its presence leads to the global solar (p-mode or 5 minutes) oscillations, which are subjects of extensive investigations in helioseismology. Furthermore, the existence of

cutoffs for propagation of acoustic and other waves in the solar atmosphere has become important for understanding the origin of chromospheric (3 and 7 minutes) oscillations and for transferring wave energy to heat the solar chromosphere and corona and to accelerate the solar wind. Typically, acoustic cutoff frequencies are determined theoretically and then are used to calculate their variations with height in a chosen model of the solar atmosphere (e.g., Brown & Gilliland (1994); Nagashima et el. 2014). In this Letter, we present observational results that confirm the existence of the acoustic cutoff frequency in the solar atmosphere and demonstrate its variation with atmospheric height. The observational results and theoretical predictions are compared and validity of the latter is determined.

Lamb (1909, 1910) was the first who formally introduced the concept of cutoff frequency and demonstrated that its existence in inhomogeneous media is fundamental for determining conditions for wave propagation. He considered acoustic waves propagating in an isothermal atmosphere and defined such a cutoff as the ratio of sound speed to twice density (pressure) scale height and showed that this cutoff uniquely determines a range of frequencies corresponding to either propagating or non-propagating (evanescent) waves. Lamb (1910, 1932) also studied a non-isothermal atmosphere with the temperature decreasing linearly with height and investigated the effects of this uniform temperature gradient on the acoustic cutoff frequency. It was a step in the right direction because the solar atmosphere does show gradients in temperature and other physical parameters. In numerous studies that followed Lamb's work, many attempts were made to properly define the acoustic cutoff frequency in non-isothermal media. Some of these attempts were simply based on the so-called local dispersion approach, which can be justified within the limit of the WKB approximation (Whitman 1974; Thomas 1983; Campos 1987; Subrahmanyam et al. 2003; Rossing & Fletcher 2004; Raichel 2006). In other approaches, analytical and numerical solutions to acoustic wave equations were obtained for different models of the background medium, and the solutions were used to determine the propagation conditions for acoustic waves (Moore & Spiegel 1964; Souffrin 1966; Summers 1974; Campos 1986; Morse & Ingard 1986; Salomons 2002).

Since Lamb's original work, the acoustic cutoff frequency has played an important role in all theories of acoustic wave propagation in inhomogeneous media of different structures. The cutoff has become a fundamental quantity in helioseismology, which uses the solar 5 minute oscillations to determine the internal structure of the Sun (Brown & Gilliland 1994; Brown et al. 1987; Christensen-Dalsgaard 2002), and in asteroseismology, which deals with oscillations observed on different stars (Hansen et al. 1985; Bouchy & Carrier 2001; Matthews et al. 2004; Musielak et al. 2005; Aerts et al. 2010; Fawzy & Musielak 2012). The cutoff has been used to study atmospheric oscillations on the Sun (Brown et al. 1987; Deubner & Gough 1984; Gough 1993; Fleck & Schmitz 1993; Schmitz & Fleck 1998; Musielak et

al. 2006; Routh & Musielak 2014), Earth (Suda et al. 1998), Jupiter (Rhie & Romanowicz 2004), and other planets (Deming et al. 1989). Moreover, the concept of the cutoff has been extended to magnetohydrodynamic waves (Kobayashi & Nishida 1998; Murawski & Musielak 2010; Routh et al. 2013; Perera et al. 2015). Admittedly, the cutoff frequency and its variation over a solar cycle were estimated for the transition between p-modes and pseudo-modes by Jiménez (2006) and Jiménez et al. (2011) based on intensity and velocity data from the instruments VIRGO and GOLF, respectively, on board the Solar and Heliospheric Observatory. Nonetheless, despite its wide range of applications, the existence of this cutoff has not yet been directly verified by solar multi-wavelength observations from a single device; the fact that its existence is required by helioseismology is only indirect evidence. Moreover, to the best of our knowledge, no observations to the date have revealed variations of the cutoff in the solar atmosphere. Therefore, the main goal of this Letter is to present observational evidence for the existence of the acoustic cutoff in the solar atmosphere and for its variations with the atmospheric heights.

We performed observations using the HELioseismological Large Regions Interferometric DEvice (HELLRIDE) operating on the Vacuum Tower Telescope (VTT) located at Tenerife. The obtained observational results are compared to theoretical predictions made by using five acoustic cutoff frequencies commonly used in helioseismology and asteroseismology. The comparison shows significant discrepancies between the data and the theoretical predictions. Because of the discrepancies, we suggest that either major revisions of the existing methods of finding acoustic cutoff frequencies are required or even that new methods must be developed that would much better account for the physical picture underlying the concept of cutoff frequencies in inhomogeneous media.

This Letter is organized as follows: our observational data and methods to analyze them are described in Sect. 2; selected acoustic cutoff frequencies are presented in Sect. 3; comparison of theoretical results to the observational data is discussed in Sec. 4; and our conclusions are given in Sec. 5.

2. Observations and data analysis

Time series of sequential multi-height observations of the solar atmosphere were recorded by using the HELLRIDE in the spectroscopic mode. The HELLRIDE instrument, originally designed and developed at the Kiepenheuer-Institut für Sonnenphysik (KIS) in Freiburg, Germany, has unique abilities to precisely track the propagation of acoustic waves through the solar atmosphere (Staiger 2011). The spectral line formation strongly depends on temperature; therefore, to measure the velocity signal of the solar plasma motion at many different

atmospheric heights, it is needed to look at the Sun at various wavelengths. In practice, this is achieved by mounting into the device a number of narrowband interference pre-filters, each with a different wavelength range. Since the formation height of each spectral line depends explicitly on the physical conditions of the plasma at different temperatures, various spectral lines can be observed corresponding to different heights in the solar atmosphere.

The quiet-Sun measurements were done by using 10 spectral lines. Measurements with nine of them fully covered the solar photosphere and lower chromosphere, corresponding to the atmospheric heights in ranging from 250 km to about 1700 km above the solar surface (see Figure 1 and Table 1). The measurements also contain the terrestrial iron line Fe I 6302$\mathring{A}$, used for device calibration. The HELLRIDE field of view is 100 by 100 arcsec and has a spatial resolution of 0.2 arcsec/pixel. With a high temporal cadence of 27.7 s and the total time measurement of T=8 hr, it is possible to investigate waves with folding frequencies up to 18 mHz. The observations were performed using 2D spectroscopic scans with many spectral ranges, which allowed us to probe the solar atmosphere very accurately and to obtain sufficient information about the structure and physical conditions that prevail at each atmospheric height; note that the average height separation for the observations was between 100 km and 200 km.

Based on the recorded time series as a function of position x on the Sun and time t, we determined the power spectra by employing a 3D Fourier transform of our velocity data cubes for all spectral lines over the atmospheric heights of 2000 kilometers (see Figure 1). The Fourier transform of the measured velocity signal $V_{\mathrm{LoS_i}}(\lambda_i, x, t)$, which is a complex number in each wavelength λ_i with $i = 1, \ldots, 9$, is defined as

$$F_{V_i}(\omega, k, \lambda_i) = \frac{1}{T} \int_{-T/2}^{T/2} e^{-i(k\cdot x+\omega t)} V_{\mathrm{LoS_i}}(\lambda_i, x, t)\, dt = \hat{V}_i \cdot e^{-i\phi_{V_i}} \ . \tag{1}$$

The density function $F_{V_i}(\omega, k, \lambda_i)$ gives the energy per unit frequency and wave vector k. Using the dependence that $\omega \cdot t = \phi$, we can describe by this function the phase ϕ of a signal. The spectral energy density or periodogram of the signal $V_{\mathrm{LoS_i}}(\lambda_i, k, t)$ is the square modulus of the Fourier transform

$$P_{V_i}(\omega, k, \lambda_i) = \mid F_{V_i}(\omega, k, \lambda)_i \mid^2 \ = \mid \hat{V}_i \cdot e^{-i\omega t} \mid^2 . \tag{2}$$

The obtained periodogram gives the frequency and wave vector dependence of the signal and allows identification of the frequency regions of the largest spectral energy density. The same definition for the periodogram is used for all recorded velocity signals $V_{\mathrm{LoS_j}}(\lambda_j, x, t)$ with $j = 1, \ldots, 9$. A two-dimensional power spectrum $S_{V_i}(\omega, \lambda_i)$ (see Figure 1) is obtained

by averaging over all orientations of the wave vector k, resulting in a power spectrum being a function of harmonic degree $l =\mid k \mid R_\odot$, with $R_\odot$ being the solar radius, and independent of azimuthal order m. From the individual Fourier transforms, we calculate all cross-coherence functions and determine the cross-spectra (Equation (3)) and the phase difference spectra $\delta\phi_{ij}$ between two different signals $V_{\mathrm{LoS_i}}(\lambda_i, x, t)$ and $V_{\mathrm{LoS_j}}(\lambda_j, x, t)$ by taking the argument of the cross-spectrum $Arg(C_{ij}(\omega))$, which is a real number within the range $[-\pi, +\pi]$, and given by

$$C_{ij}(\omega) = \langle F_{V_i}(\omega, k, \lambda_i) \cdot (F_{V_j}(\omega, k, \lambda_j))^* \rangle_k = \hat{C}_{ij} \cdot e^{-i(\phi_{V_i} - \phi_{V_j})} \ , \tag{3}$$

where $\langle\rangle_k$ indicates averaging over all orientations of the wave vector and * is the complex conjugate.

The phase can only be evaluated for cases where the coherence

$$\mid Coh_{ij}(\omega) \mid = \frac{\mid C_{ij}(\omega) \mid}{\sqrt{\mid S_{V_i}(\omega, \lambda_i) \mid^2 \cdot \mid S_{V_j}(\omega, \lambda_j) \mid^2}} \tag{4}$$

is significant. The coherence $Coh_{ij}(\omega)$ defined by Equationn(4) is a function of frequency with values in the range $[0, 1]$. A significant coherence for a given frequency is a clear indication of linear dependence of the two signals at this frequency. The level of significance or confidence interval for the coherence (see Figure 3) was calculated by the standard zero coherency test (Equation(5)), where F is the test for residual sum of squares

$$F = \frac{2n \cdot \mid Coh_{ij}(\omega) \mid}{(1 - \mid Coh_{ij}(\omega) \mid^2)} \ , \tag{5}$$

with n being the parameter associated with the width of the smoothing window. With the smoothing we used, the coherence is significant (at the 95% level) if it is > 0.35. This confidence level is indicated as a contour line in Figure 3. Values of coherence below this threshold are considered as non-significant. In the case of a non-significant coherence, the phase is a random number from the interval $[-\pi, \pi]$. Due to correlated background noise, significant coherence is present outside the p-mode region, too. However, the coherence is highest and close to 1 in the region of solar oscillations, in which we are interested in.

We established the phase difference information $\delta\phi_{ij}$ about the propagation of acoustic waves at different heights in the solar atmosphere (see Table 1). If the phase difference is near zero $\delta\phi_{ij} \approx 0^\circ$ at given frequencies, the observed oscillations are identified as standing waves, and if the phase shift is not zero $\delta\phi_{ij} \neq 0^\circ$, then the waves are propagating waves; negative values of the phase shift imply the upward direction of wave propagation. Our observations

clearly show that in the solar photosphere the oscillations with maximum power are those with frequencies equal to 3.5 mHz, whereas in the solar chromosphere higher frequencies start to become important (see Figs 2 and 4). Fig. 4 presents a vertical cut through two chosen phase spectra (Figure 2) at a harmonic degree of l=301. It exhibits a general decreasing trend in the phase shift away from the position of the acoustic cutoff. To compute more exact values of this point at which the phase starts to turn negative, we averaged over the interval between $l = 180$ and 301. A vanishing phase then identifies a standing wave in the given range of the atmosphere. The values of the cutoff frequencies are therefore given with a tolerance of 10° in the phase shift (error bars in frequency). The results for all lines are presented in Figure 5 (top panel)

The observationally established variations of the acoustic cutoff frequency with atmospheric height in the solar atmosphere are presented in Figure 5 (lower panel), which demonstrates that the cutoff initially increases in the solar chromosphere before its variations level off in the upper parts of the considered atmosphere. This particular behavior of the cutoff frequency is caused by gradients of physical parameters in the solar atmosphere. The presented results have profound implications on theories that were previously used to determine acoustic cutoff frequencies for the solar atmosphere. Thus, we compare the acoustic cutoff frequencies obtained by different theoretical methods to our observational results and determine the validity of those theoretical predictions. The comparison is done in Figure 5 (lower panel), which clearly shows the discrepancies between the theoretical and observational results. We comment on these discrepancies after we describe five theoretically obtained acoustic cutoff frequencies selected for this paper.

3. Selected acoustic cutoff frequencies

Since the solar atmosphere is highly inhomogeneous, it is expected that the acoustic cutoff frequency will be a local quantity. However, the problem is that different theories predict different dependences of the cutoff on atmospheric height and that so far there has been no way to verify which theoretical prediction is the correct one. With our observational results, we can for the first time discriminate between different theories and identify the best theoretical method of finding the acoustic cutoff frequency in the non-isothermal solar atmosphere. We have chosen five different but commonly used acoustic cutoff frequencies from the literature, evaluated their values in the solar atmosphere represented here by the so-called VAL C model (Vernazza et al. 1981), and compared them to our observational results (see the bottom panel of Figure 5). Our choices of acoustic cutoff frequencies are based on the acoustic wave equations obtained for the velocity perturbations. The main reason for these

choices is the fact that in our observations we primarily measured velocity perturbations of the acoustic waves propagating in non-magnetic regions of the solar atmosphere. The selected acoustic cutoff frequencies are given in the following.

First, we consider Lamb's original cutoff frequency (Lamb 1910) but assume that its value changes locally with atmospheric height

$$\Omega_1(z) \equiv \omega_a(z) = \frac{C_s(z)}{2H_p(z)} \ , \tag{6}$$

where C_s is the sound speed, H_p is the pressure scale height, and z is the atmospheric height.

An important modification of Lamb's acoustic cutoff frequency was given by Gough (1993), who derived the acoustic cutoff by including the perturbation of the gravitational potential and the effects of spherical geometry. A simplified version of Gough's (1993) original work was given by Deubner & Gough (1984, see their Equation 2.4), who neglected the perturbation in the gravitational potential (i.e. applying the Cowling approximation) and the effects of spherical geometry and obtained

$$\Omega_2(z) = \frac{C_s(z)}{2H_\rho} \left[1 - 2\frac{dH_\rho(z)}{dz}\right]^{1/2} \ , \tag{7}$$

where H_ρ is the density scale height. It must be noted that this formula is commonly used in helioseismology and asteroseismology.

Then, we choose two acoustic cutoff frequencies derived by Schmitz & Fleck (1998)

$$\Omega_3(z) = \omega_a(z) \left[1 + 2\frac{\omega_s(z)}{\omega_a(z)}\right]^{1/2} \ , \tag{8}$$

and

$$\Omega_4(z) = \left[\Omega_3^2(z) + \frac{1}{4}\omega_s^2(z) - \frac{1}{2}C_s(z)\omega_s'(z)\right]^{1/2} \ , \tag{9}$$

where ω_s and ω_s' are the first and second derivatives of C_s with respect to z. The main difference between these two cutoffs is that $\Omega_4(z)$ was obtained by using the Lamb transformation $d\tau = dz/C_s(z)$.

Finally, we follow Musielak et al. (2006), who derived the wave equations for both the velocity and pressure perturbations and showed how to obtain the resulting acoustic cutoff frequency by introducing two new concepts, the so called critical and turning-point frequencies. Since the above cutoffs were derived for the velocity perturbations only, we identified the turning-point frequency obtained for the velocity perturbations by Musielak et al. as the acoustic cutoff frequency and use it here in our calculations. The result is

$$\Omega_5(z) = \Omega_{tp}(z) = \left[\Omega_{crit}^2(z) + \Omega_{tau}^2(z)\right]^{1/2} \ , \tag{10}$$

where the critical frequency is given by

$$\Omega^2_{crit}(z) = \omega^2_a(z) + \omega^2_s(z) + 4\omega_a(z)\omega_s(z) - C_s(z)\omega'_s(z) \ , \tag{11}$$

and

$$\Omega^2_{tau}(z) = \frac{1}{4}\left[\int^z \frac{d\tilde{z}}{c_s(\tilde{z})}\right]^{-2} \ . \tag{12}$$

Physical meaning of these five selected acoustic cutoff frequencies is that their values at a given atmospheric height determine the frequency that acoustic waves must have in order to be propagating at the height. In the following, we adopt the above formulas to compute their variations in our solar atmospheric model and compare these variations with our observational results. The comparison allows us to verify the validity of the selected expressions for acoustic cutoff frequencies in the solar atmosphere.

4. Comparison of theoretical results to observational data

We used the expressions for acoustic cutoff frequencies presented in the previous section to calculate variations of these cutoffs in the solar atmosphere, which is assumed here to be described by the VAL C model (Vernazza et al. 1981). The results of our calculations are compared to our observations in the bottom panel of Fig. 5. First, the cutoffs Ω_1 and Ω_3 seem to be inconsistent with the observational data in the entire considered model. Second, it is interesting to notice that the three cutoff frequencies Ω_2, Ω_4, and Ω_5 have values too similar to be distinguished in the presented plots and that for the atmospheric heights ranging from approximately 350 km to 500 km they match the observational results rather well. Third, at the photospheric heights below 350 km and the chromospheric heights above 500 km, the discrepancies between these three cutoffs and the observational results remain significant, which clearly shows that none of these cutoffs can correctly account for the observed variations of the acoustic cutoff in the entire solar atmosphere. Based on this comparison, we conclude that significant improvements in methods of finding acoustic cutoff frequencies in the solar atmosphere as well as in other inhomogeneous media are urgently needed. These improvements may require much better understanding of the basic physics underlying the concept of cutoff frequencies in inhomogeneous media.

5. Conclusions

We presented the direct observational evidence for the existence of acoustic cutoff frequency in the solar atmosphere and for its variations with the atmospheric height by per-

forming solar observations with the HELLRIDE instrument operating on the VTT located on Tenerife. Our observational data were used to critically examine theoretical methods of finding acoustic cutoff frequencies available in the literature. We identified the cutoffs that match the observational data in a certain range of the solar atmosphere, but also demonstrated that no cutoff frequency currently available can fully match the data for the entire solar atmosphere. Based on this result, we suggest that the discovered inconsistency requires either major revisions of the existing methods of finding cutoff frequencies or developing new methods that would much better account for the physical picture underlying the concept of cutoff frequencies in inhomogeneous media.

Acknowledgments The authors thank Reiner Hammer for useful discussions and Vigeesh Gangadharan for commenting on the manuscript. This work has been supported by the German Academic Exchange Service DAAD (A.W.), NSF under the grant AGS 1246074 (Z.E.M.), and by the Alexander von Humboldt Foundation (Z.E.M.). The research leading to these results has received funding from the European Research Council under the European Union's Seventh Framework Program (FP/2007-2013)/ERC grant Agreement No. 307117. MR, JS and AW acknowledge support from the Solarnet project, which has received funding by the European Commissions FP7 Capacities Programme for the period 2013 April 2017 March under the grant Agreement No. 312495.

REFERENCES

Aerts, C., Christensen-Dalsgaard, J., Kurtz, D., 2010, Asteroseismology (Springer Science and Business Media, New York)

Bouchy, F., Carrier, F., 2001, A&A, 374, L5

Brown, T.M., Gilliland, R.L., 1994, Ann. Rev. Astron. Astrophys., 32, 37

Brown, T.M., B.M. Mihalas, B.M., & Rhodes, J. 1987, in Physics of the Sun, Ed. Peter A. Sturrock, Vol. 1, 177

Bruls, J.H. M. J.,Lites, B. W., Murphy, G.A.1991, in L.November (ed.), Solar Polarimetry, Proc. 11th Sacramento Peak Workshop, NSO, Sunspot, New Mexico

Campos, L.M.B.C., 1986, Rev. Mod. Phys., 58, 117

Campos, L.M.B.C., 1987, Rev. Mod. Phys., 59, 3363

Christensen-Dalsgaard, J., 2002, Rev. Mod. Phys., 74, 1073

Deming, D., Mumma, M. J., Espenak, F., et al., 1989, Astrophys. J. 343, 456

Deubner, F.-L., Gough, D.O., 1984, Ann. Rev. Astron. Astrophys., 22, 539

Fawzy, D.E., Musielak, Z.E., 2012, MNRAS, 421, 159

Fleck, B., Schmitz, F., 1993, A&A, 273, 487

Gough, D.O., 1993, Astrophysical Fluid Dynamics, Eds. J.-P. Zhan and J. Zinn-Justin, Les Houches, Elsevier, Amsterdam, p. 399

Hansen, C.J., Winget, D.E., Kawaler, S.D., 1985, ApJ, 297, 544

Jiménez, A., 2006, ApJ, 646, 1398

Jiménez, A., García, R.A., Pallé, P.L.,2011, ApJ, 743, 99

Kobayashi, N., Nishida, N., 1998, Nature 395, 357

Lamb, H., 1909, Proc. Lond. Math. Soc., 7, 122

Lamb, H., 1910, Proc. R. Soc. London, A, 34, 551

Lamb, H., 1932, Hydrodynamics (Dover, New York)

Matthews, J. M., Kusching, R., Guenther, D. B., et al., 2004, Nature, 430, 51

Moore, D.W., Spiegel, E.A., 1964, ApJ., 139, 48

Morse, P.M., Ingard, K.U., 1986, Theoretical Acoustics (Princeton Uni. Press, Princeton)

Murawski, K., Musielak, Z.E., 2010, A&A, 518, A7

Musielak, Z.E., Musielak, D.E., Mobashi, H., 2006, Phys. Rev. E 73, 036612-1

Musielak, Z.E., Winget, D.E., Montgomery, M., 2005, ApJ, 630, 506

Nagashima, K., Lptien, B., Gizon, L., et al., 2014, Sol. Phys., 289, 3457

Perera, H., Musielak, Z.E., Murawski, K., 2015, MNRAS, 450, 3169

Raichel, D.R., The Science and Applications of Acoustics (Springer Science and Business Media, New York)

Rhie, J., Romanowicz, B., 2004, Nature 431, 552

Rossing, T.D., Fletcher, N.H., 2004, Principles of Vibrations and Sound (Springer-Verlag, New York)

Routh, S., Musielak, Z.E., 2014, Astron. Nachr., 335,1043

Routh, S., Musielak, Z.E., Hammer, R., 2013, ApJ, 763, 44

Salomons, E.M., 2002, Computational Atmospheric Acoustics (Kluwer Acad. Publ., Dordrecht)

Schleicher, H., 2015, private communication

Schmitz, F., Fleck, B., 1998, A&A, 337, 487

Souffrin, P., 1966, AnAp., 39,55

Staiger, J., 2011, A&A, 535, A83 (2011).

Subrahmanyam, P.B., Sujith, R.I., Lieuwen, T.C., 2003, J. Vibration and Acoustics, 125, 133

Suda, N., Nawa, K., Fukao, Y., 1998, Science, 279, 2089

Summers, D., 1976, Quart. J. Mech. Appl. Math., 29, 117

Thomas, J.H., 1983, Ann. Rev. Fluid Mech., 15, 321

Whitman, G.B., 1974, Linear and Nonlinear Waves (Wiley, New York)

Wiśniewska, A.; Roth, M.; Staiger, J., 2015, Central European Astrophysical Bulletin, 39, 101

Vernazza, J.E., Avrett, E.H., Loeser, R., 1981, ApJ Sup. 45, 635

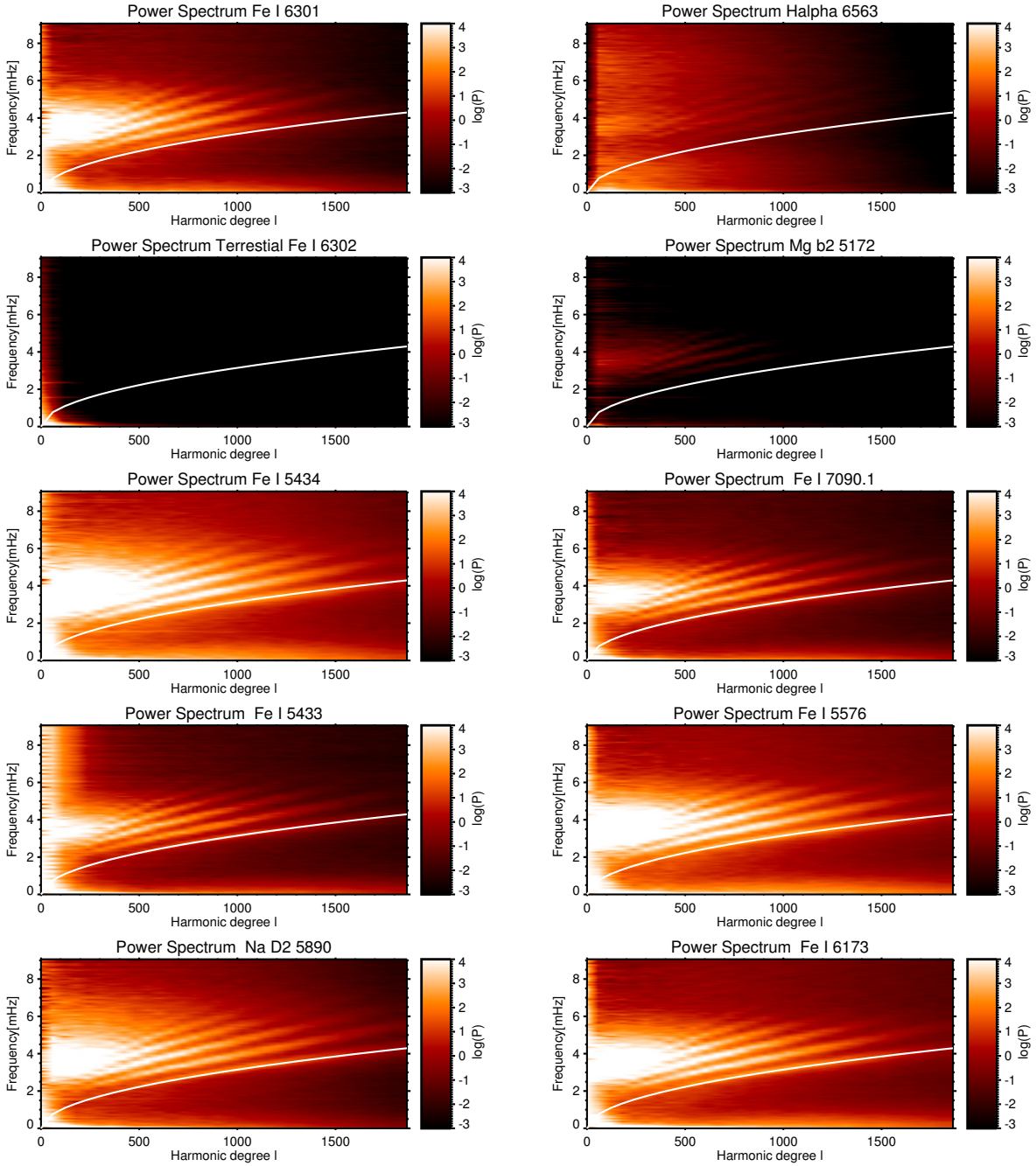

Fig. 1.— Measured velocity signal of the solar atmospheric oscillations is shown as a power spectrum of spectral density $log_{10}P$ for the average angular m-number, and is plotted vs. the harmonic degree l and frequency ν. The observational results are presented for 10 spectral lines. Line 630.2 nm is the control terrestrial line used only for device calibration. The formation heights of those lines in the solar atmosphere are given in Table 1. The white solid line represents the theoretical location of the fundamental f- mode.

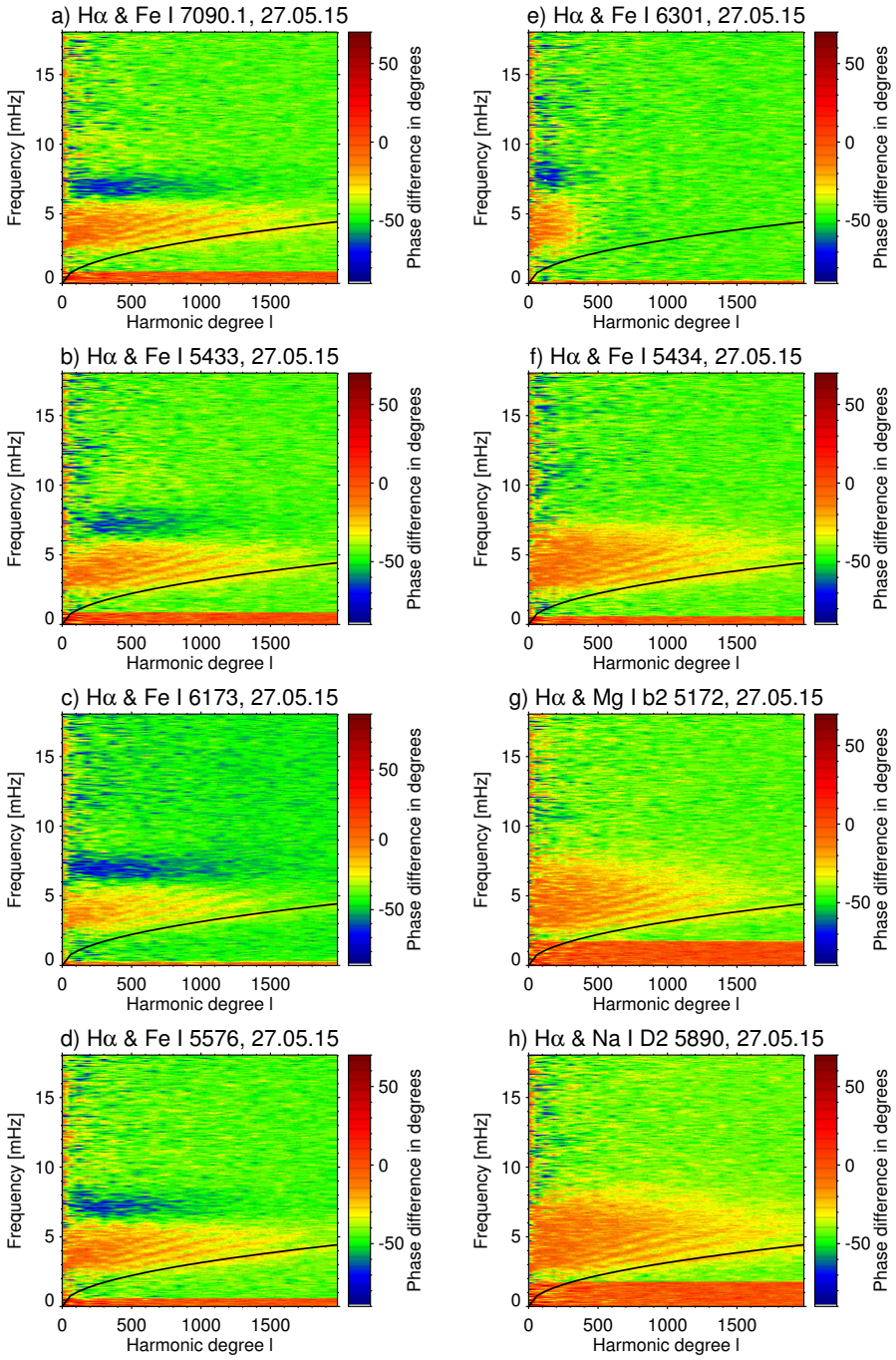

Fig. 2.— Phase diagrams for the Hα line cross-correlated with the eight other chosen spectral lines. These diagrams show phase differences between acoustic waves as measured at various heights (cf. Table 1.) for the observed quiet-Sun region. The presented results are direct observational evidence for the existence of a cutoff frequency in the solar atmosphere and also show its variations with height. Colors indicate the negative/positive phase shifts of the acoustic wave speed at a given frequency. The transition between standing waves ($\delta\phi = 0°$) and propagating waves ($\delta\phi = 90°$) uniquely defines the acoustic cutoff frequency. The solid black line in each panel represents the location of the f-mode in each phase diagram.

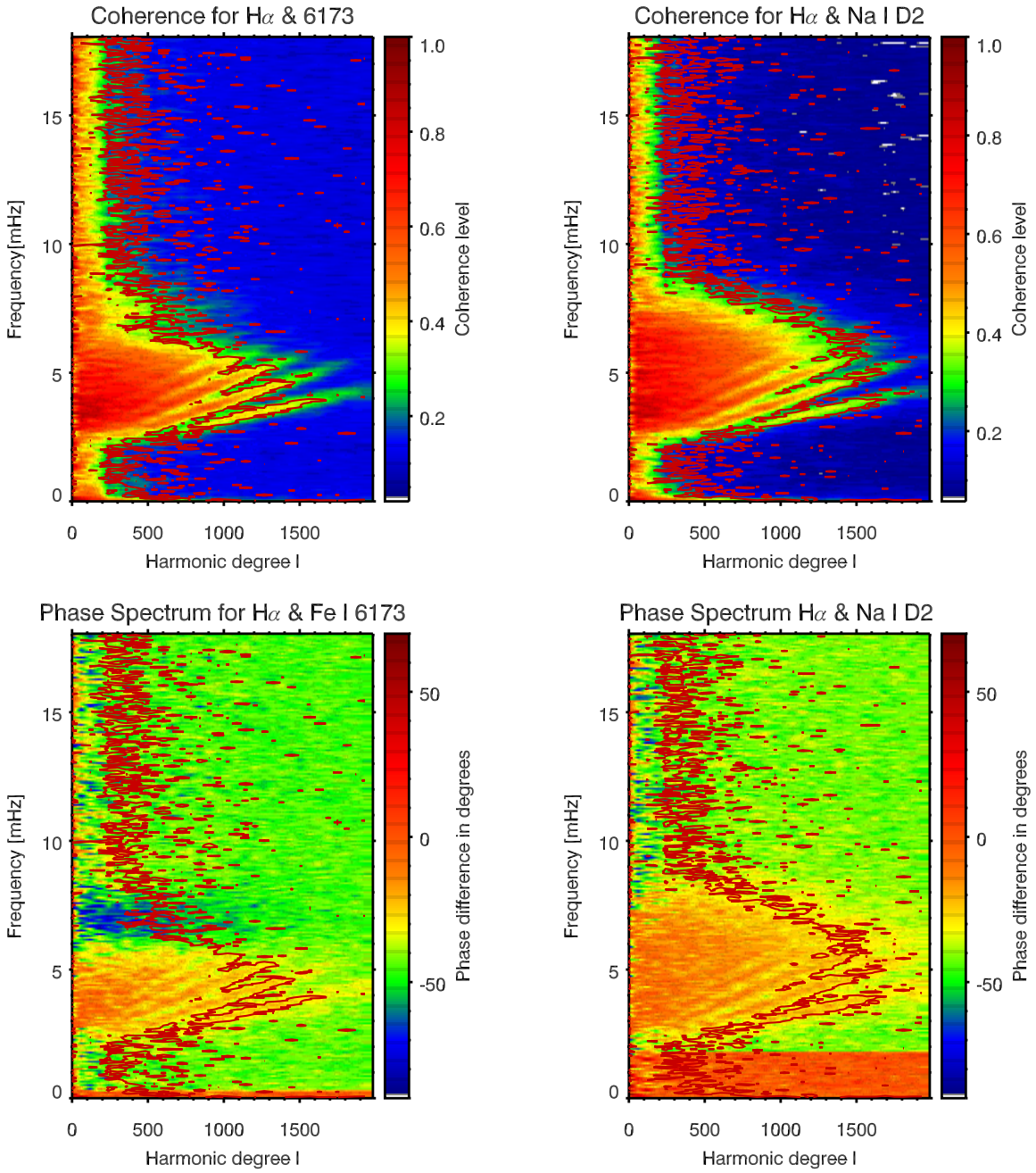

Fig. 3.— Top panels: coherence function calculated for Hα with the lines Fe I 6173$\mathring{A}$ (left) and Na I D_2 (right). The red contour marks the significance level for the coherence. The coherence is therefore significant for frequencies 2 mHz $< \nu <$ 8 mHz below a harmonic degree $l \approx$500 in both cases. Bottom panels: phase difference for the same pairs of spectral lines with the red contour representing the significance level of the coherence.

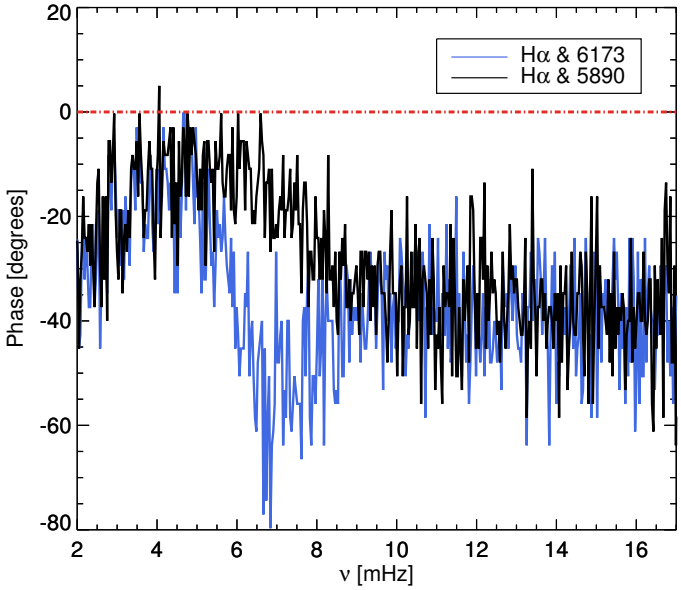

Fig. 4.— Vertical cut through the phase spectra at l=301 for the two pairs of spectral lines selected for Fig. 3. Blue solid line: Phase difference between Hα and Fe I 6173$\mathring{A}$ formed at a height of $\approx$ 300 km. Black solid line: Phase difference between Hα and Na I D2 formed at $\approx$ 900 km. The observed decreasing of the phase difference is significant and starts for waves propagating from the photospheric level at around ν = 5 mHz and for waves propagating from chromospheric region at around ν =7 mHz.

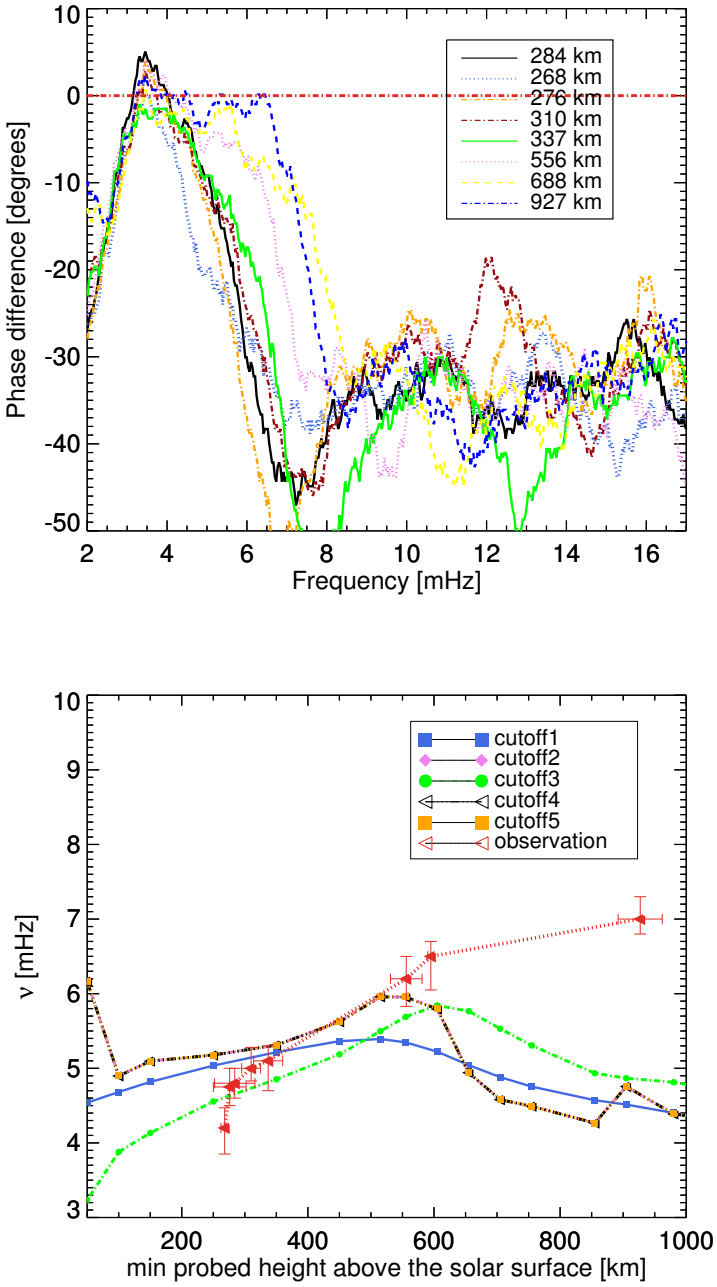

Fig. 5.— Results presented in Figure 2 were used here to plot (top panel) the averaged phase variations for harmonic degrees between $180 \leq l \leq 301$ for different atmospheric heights in kilometers. Bottom panel: dependence of the observationally and theoretically established acoustic cutoff frequencies as a function of height in the solar atmosphere. The error bar related to specific values of the observed acoustic cutoff frequency is calculated from error propagation of the 10° error in the phase shift. The estimated atmospheric heights are given in Table 1. Note that cutoff1 = Ω_1, cutoff2 = Ω_2, and so on.

Table 1. Formation heights for the 10 observed spectral lines formed in the Solar Atmosphere. Note.The formation height of the terrestial iron line 6302 is not discussed. An LTE model was used for the photospheric Fe I spectral lines and a non-LTE model for the three other chromospheric lines. References for the first and second Fe I line and for the last and second to the last Fe I line are Bruls et al. (1991). For the third, fourth and sixth line, the references are in Wiśniewska et al. (2015). Finally, for the fifth and seventh line, the references are in Vernazza et al. (1981) and in Schleicher (2015, private communication), respectively

Spectral Line	Wavelength in $\AA$	Lande g-factor	Formation Height
Fe I	6302	-	-
Fe I	6301	1.669	337 ± 23
Fe I	5434	0.0	556 ± 25
Fe I	5433	0.0	268 ± 6
Na I D_2	5890	-	927 ± 35
Hα	6562.7	1.048	1200-1700
Mg I b_2	5172	-	595 ± 5
Fe I	6173	2.499	276 ± 26
Fe I	5576	0.0	310 ± 15
Fe I	7090.1	0.0	284 ± 32